J. SE Asian Appl. Geol., Jul–Dec 2011, Vol. 3(2), pp. 93-102

GROUND MOVEMENT PREDICTION DUE TO BLOCK CAVING MINING GEOMETRY USING GIS

Agung Setianto*[1] and Eman Widijanto[2]

[1]*Geological Engineering Department, Faculty of Engineering, Gadjah Mada University*
[2]*Rock Mechanics Engineer PT Freeport Indonesia, Timika*

Abstract

Large scale block cave mining has been operated for over 30 years in the Erstberg Mining District in the province of Papua, Indonesia. The ore body is divided into four vertically stacked ore bodies: Gunung Bijih Timur (GBT), Intermediate Ore Zone (IOZ), Deep Ore Zone (DOZ), and Deep Mill Level Zone (DMLZ). The GBT and IOZ mines were closed on 1993 and 2003, DOZ mine is in its peak production performance 80 ktpd, and DMLZ mine is still in the development stage to prepare mine infrastructures. This situation generates gradual downward settling of the surface or subsidence. Significant deformation changes at the surface by block caving subsidence could damage the mine's infrastructures in surface and underground and also affect geological structures overlying the mining areas which may result in surface impacts on the natural geomorphology and land use.

In this paper, integrated system based on Geographic Information System (GIS) platform applied to predict ground movements due to underground mining. Deep Ore Zone (DOZ) block cave mine is studied for subsidence prediction. The mining extraction thickness model is obtained from height of draw (HOD) observed data. Subsidence Engineering Handbook (SEH) of empirical model and measured data from mining fields is used for subsidence calculation parameters. The calculations were performed in GIS. The maximum vertical displacement has been predicted about 12m by means of full caving mining method.

Keywords: *Ground movements, block caving, GIS, underground mining, and subsidence*

1 Introduction

Subsidence can be defined as the sudden sinking or gradual downward settling of the earth's surface with little or no horizontal motion. The movement is not restricted in rate, magnitude, or area involved. Subsidence may be caused by natural geological processes, such as solution, thawing, compaction, slow crustal warping, or withdrawal of fluid lava from beneath a solid crust; or by human activity, such as subsurface mining or the pumping of oil or groundwater (American Geological Institute, 1996).

The phenomena of ground movement due to block caving is an important issue since it will impact the existing critical mine infrastructures for both surface and underground areas, i.e. electrical poles, orepasses, ventilation shafts, and surface roads. The Ertsberg East Skarn System (EESS) is a calcium-magnesium silicate skarn (Coutts *et al.*, 1999) which is divided into different extraction levels: Gunung Bijih Timur (GBT), Intermediate Ore Zone (IOZ), Deep Ore Zone (DOZ), and Deep Mill Level Zone (DMLZ). However, the GBT and IOZ block cave was depleted in 1993 and in 2003 (Szwedzicki et al, 2004) respectively. Currently, the DOZ block cave is the largest sin-

*Corresponding author: A. SETIANTO, Geological Engineering Department, Faculty of Engineering, Gadjah Mada University. Jl. Grafika No. 2 Yogyakarta 55281 INDONESIA. E-mail: agung.setianto@gmail.com

gle underground block cave mine activity in the world.

The production level of the DOZ block cave is at 3126 level lies at a depth of about 1200 meters below the surface. In DOZ block caving, the full orebody or an approximately equidimensional block of ore is undercut fully to initiate caving. The undercut zone is drilled and blasted progressively and some broken ore is drawn off to create a void into which initial caving of the overlying ore can take place. As more broken ore is drawn progressively following cave initiation, the cave propagates upwards through the orebody or block until the overlying rock also caves and surface subsidence occurs.

2 DOZ block caving

2.1 Geological information in the vicinity of DOZ

The geological information map such as fault lines and mineral distributions in vicinity of DOZ is shown in Figure 1. The sedimentary rocks in the subsurface that hosted the DOZ deposit have been hydrothermally altered into various calc-silicate mineral assemblages. The main structural features in the vicinity of DOZ area are the west-northwest trending, steeply dipping Ertsberg 1 fault, Ertsberg 2 fault, Ertsberg 3 fault and the Ertsberg 4 fault to the south. These faults have kilometer-scale, reverse-sense offsets. This contact strikes roughly north/south, has vertical dip, and cuts the WNW trending Ertsberg Fault system. Bedding, preserved in some alteration assemblages, dips 50 – 55 degrees to the northeast.

2.2 Current subsidence monitoring

Basically, there are several existing monitoring to determine changes or deformation in PT Freeport Indonesia subsidence area (Figure 2). The changes of cave profile in subsurface is identified using regular cave inspection in underground drift or tunnel, Time Domain Reflectometry (TDR) cables which can identify crack or cave location based on cable fault/break position, and microseismic monitoring which can differentiate seismogenic and massive zone sur-

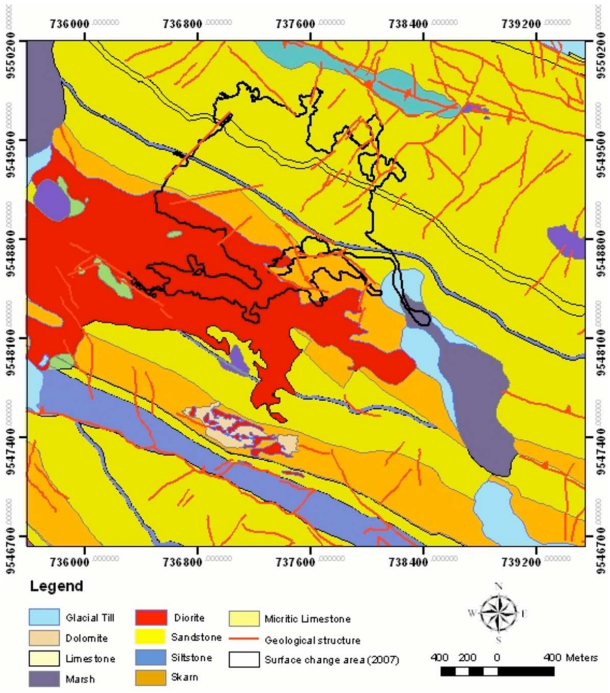

Figure 1: Sub-surface geological map, lithology distribution and the geological structure at DOZ deposit

rounding the cave area. For the changes at the surface subsidence is monitored using prism point survey to identify position or coordinate change (x, y, z) and aerial photo mapping to generate topography surface (Figure 3 and 4).

The current monitoring has limitations, especially the surface monitoring, since it depends on weather and field condition; survey pick-up and aerial photo have to be conducted in good weather.

2.3 Extraction panels and its caving model

The DOZ mine initiated caving in November 2000. Figure 4 shows the sequences of extraction area from 2000 to 2009. Starting from 2000, the extraction was progressed to the east to reduce impact of the DOZ caving on the operations of the IOZ block cave mine. After the IOZ was exhausted in 2004, caving was started towards the west. Figure 3 shows the 3D view of extraction points and its calculated extraction heights. The extraction height is obtained from height of draw (HOD) data. The HOD is the total amount of material taken during the process

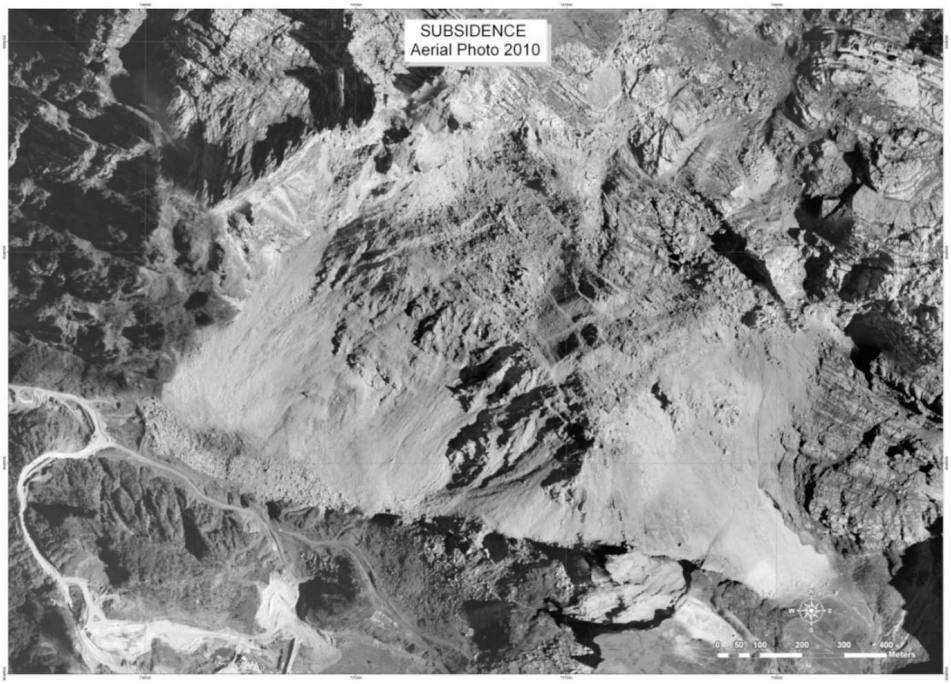

Figure 3: The subsidence aerial photo mapping which taken on 2010

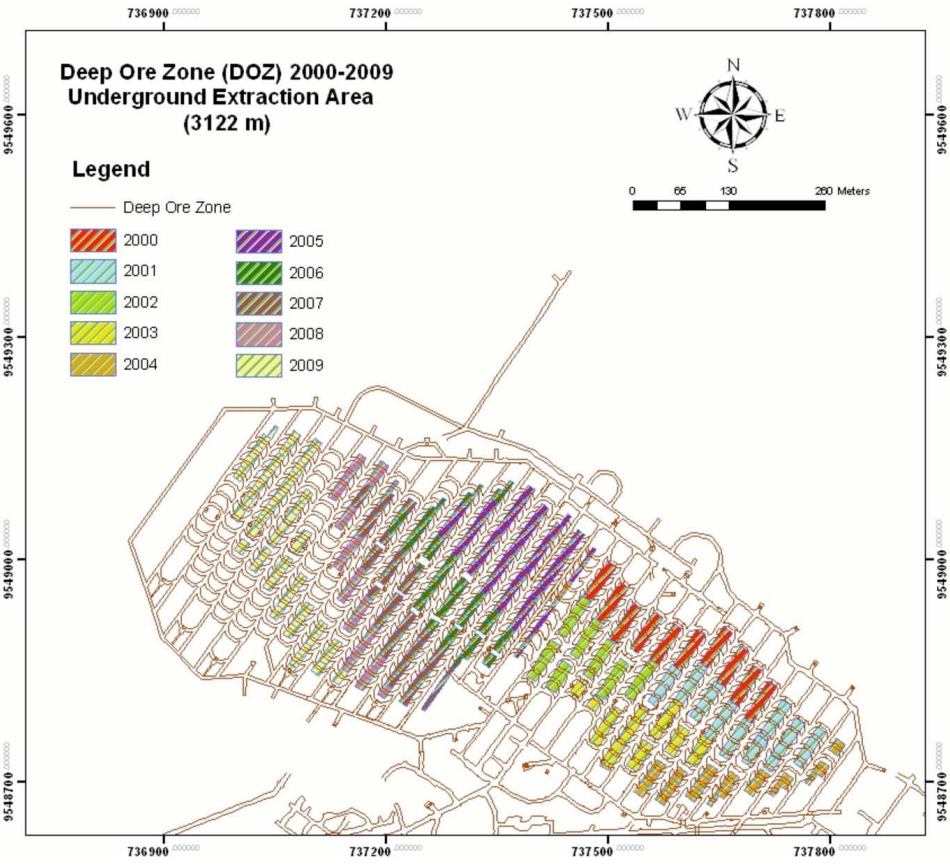

Figure 4: View of extraction area and the schedule of extraction from 2000- 2009

Figure 2: Prism monitoring at the surface subsidence

of extraction. Maximum height of extraction at points from 2000 to 2008 is about 459 m while the minimum is about 4 m.

3 Methodology of ground movement prediction

3.1 Basic Influence function model for horizontal extraction panel

According to the principle of superposition, the consequence for the extraction panel would be equal to the sum of the effects caused by those infinitesimal extraction areas. Based on the stochastic theory, the occurrence of a rock-mass movement over the extraction element may be a random event that takes place with a certain probability. An extraction with an infinitesimal unit width, length and thickness ($\partial w \partial l \partial m$) is called the extraction element. The vertical displacement of any point in the subsidence trough is called the basic influence function of vertical displacement (Se). The occurrence of the event that surface movements in an infinitesimal area; $dA = dxdy$, at horizon z, with point $P(x, y, z)$ at its center, is equivalent to the simultaneous occurrence of two events composed of a movement in the horizontal strip dx and the horizontal strip dy through P. Fundamentally, the probability can be written separately for these two events by $C(x_2)dx$ and $C(y_2)dy$, respectively, where C is the subsidence trough function. The probability for a simultaneous occurrence of these two events is:

$$P(dA) = C(x_2)dx \times C(y_2)dy = C(x_2)C(y_2)dA \tag{1}$$

The stochastic influence coefficient governs the geometric rule for distribution of subsidence owing to the extraction element. Consider a polygon extraction that both the width w and the length l of extraction and then the extraction volume is given as $w \times l \times m$ (Figure 5).

The final surface subsidence due to an extraction of finite width w and infinite length ($l \to \infty$) will be:

$$S(x) = S_{max}\left[\frac{1}{2}erf(\sqrt{\pi}\frac{x}{r_u}) - \frac{1}{2}erf(\sqrt{\pi}\frac{x-w}{r_u})\right] \tag{2}$$

Where: $r_u = (dh_u - H)/\tan\gamma$ is radius of the influence circle which controlled by the angle of draw and distance from surface point to the extraction level; and H = depth of extraction panel to surface point.

The horizontal displacement of the ground surface will be

$$v(x) = bS_{max}\left[erf\left(-\frac{\pi}{r_u^2}x^2\right) - erf\left[-\frac{\pi}{r_u^2}(x-w)^2\right]\right] \tag{3}$$

Differentiating equations of horizontal displacement produces the horizontal strain due to an extraction of finite width w :

$$\begin{aligned} e(x) &= \frac{dv(x)}{dx} = \frac{2\pi bS_{max}}{r_u} \times \\ &\left\{-\frac{x}{r_u}\exp(-\pi\frac{x^2}{r_u^2}) + \right. \\ &\left.(\frac{x-w}{r_u})\exp\left[-\pi\left(\frac{x-w}{r_u}\right)^2\right]\right\} \end{aligned} \tag{4}$$

3.2 Algorithm Implementation of prediction model in GIS

Figure 6 shows the flow chart for the algorithm of prediction analysis using GIS functions in order to calculate 3D surface movements. In the first step of GIS computational

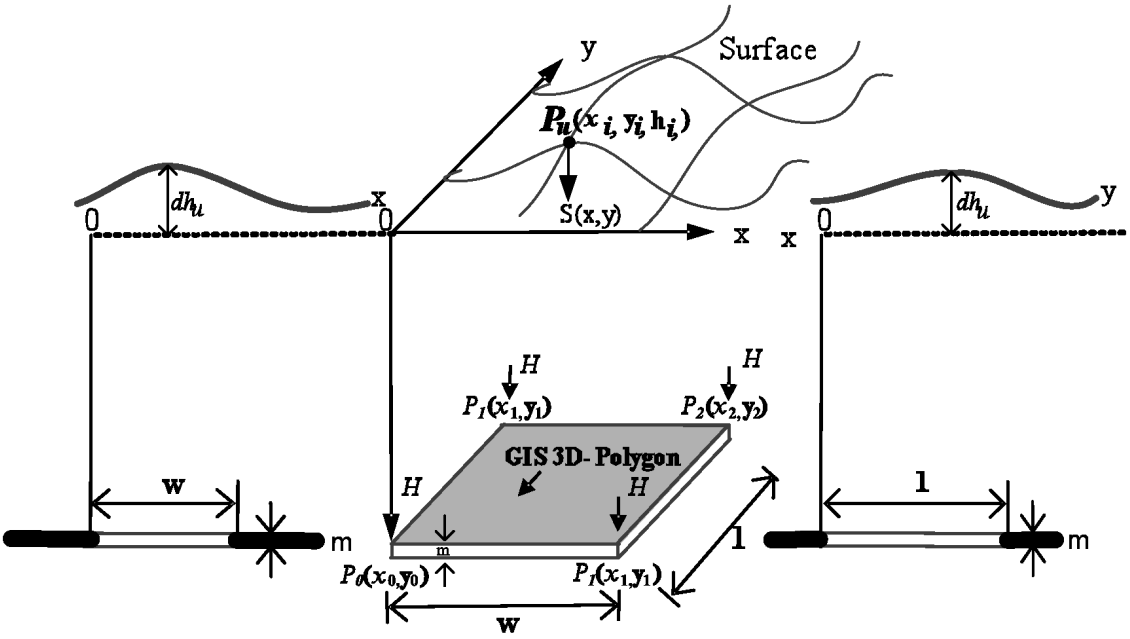

Figure 5: 3D view of a horizontal extraction and terrain surface for predicting subsidence at a surface point

process, the panel on global coordinate system is transformed into local coordinate system. The transformation coordinate panel is performed to obtain the angle direction of zone radius of the main subsidence influences. Then, a prediction of subsidence distribution is calculated in the stochastic-prediction procedures. Finally, the calculated results of subsidence are obtained according to the working panel number. All entered data (such as panels caving, calculation points, and subsidence parameters) for subsidence prediction are available by using the functions of GIS. Meanwhile, the input parameters for subsidence calculations are divided into two categories. The first parameter is the generation of surface grid points for providing calculation points at the surface, including the distance of each grid point in the x and y directions in which the number of points along the grid lines, the number of grid lines, point intervals along the grid lines, and the grid-line directions need to be established. The second parameter is entering the subsidence-calculation data, including the panel caving (panel ID), extraction thickness, subsidence factor, horizontal-movement factor, and angle of draw. By entering those data into the prediction system, the 3D movements are calculated with respect to the polygon panels.

4 Prediction of ground movement due to DOZ

4.1 Constructing 3D discrete polygons and 3D grid calculation points

There are three main processes in GIS for constructing 3D geometrical models: extraction boundary projection, cut-fill spatial analysis, and the extraction value of the raster to the vector polygon layer. Figure 7 shows the flow chart for constructing 3D extraction model which is based on the HOD data from 2000 to 2008. Entirely, there are 275 extraction points with the minimum elevation is 3,132 m and the maximum elevation is 3,580 m. In order to obtain optimum boundary model and accurate subsidence calculation by using influence function model, polygon extraction model in z direction is divided with interval 10 m.

However, small interval of polygon increases number of the total polygon and then requires more time to calculate. As a result, a 3D view of the constructed 3D discrete polygons for the

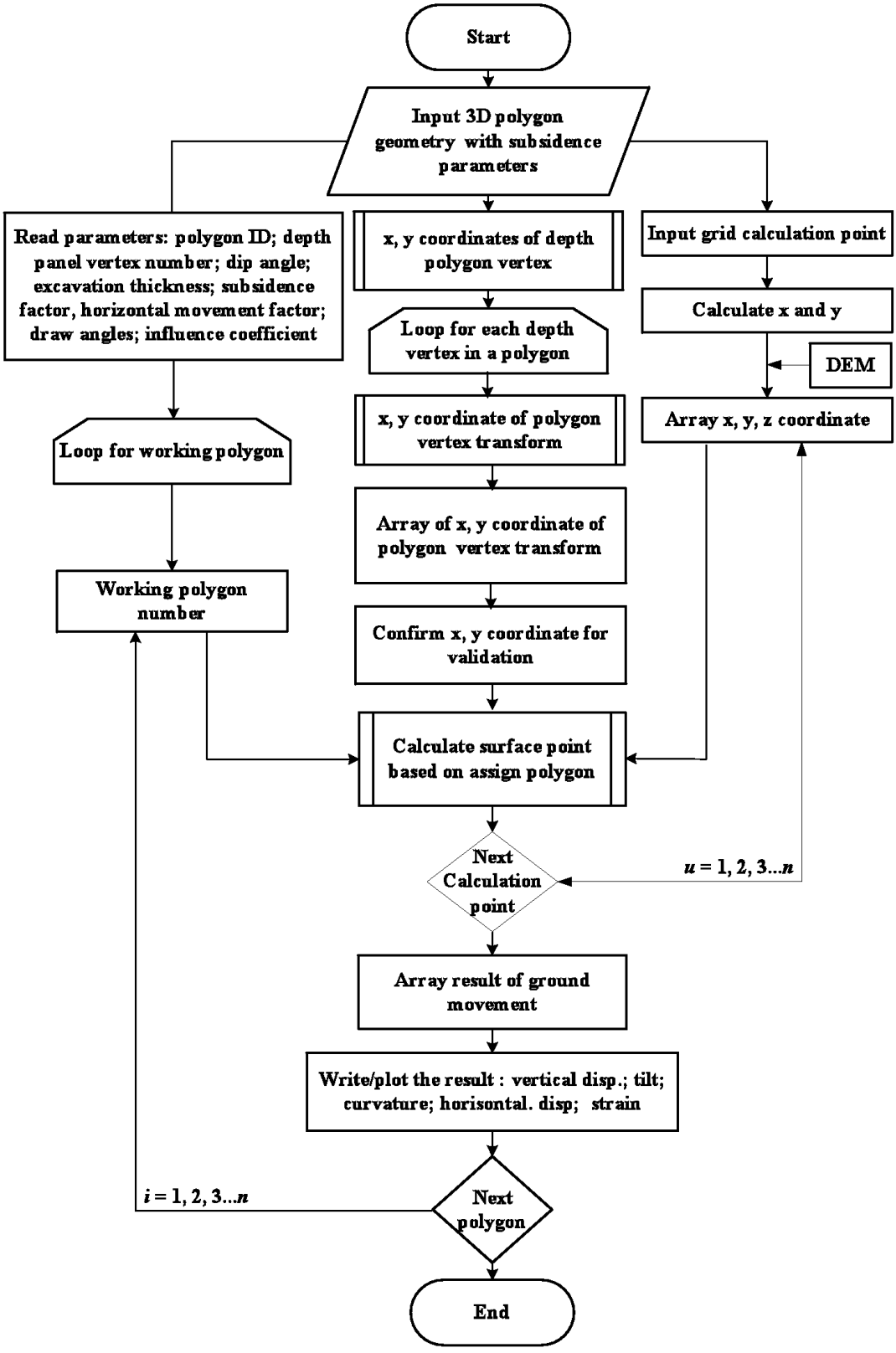

Figure 6: Flowchart improved GIS prediction model to calculate ground movement on terrain surface

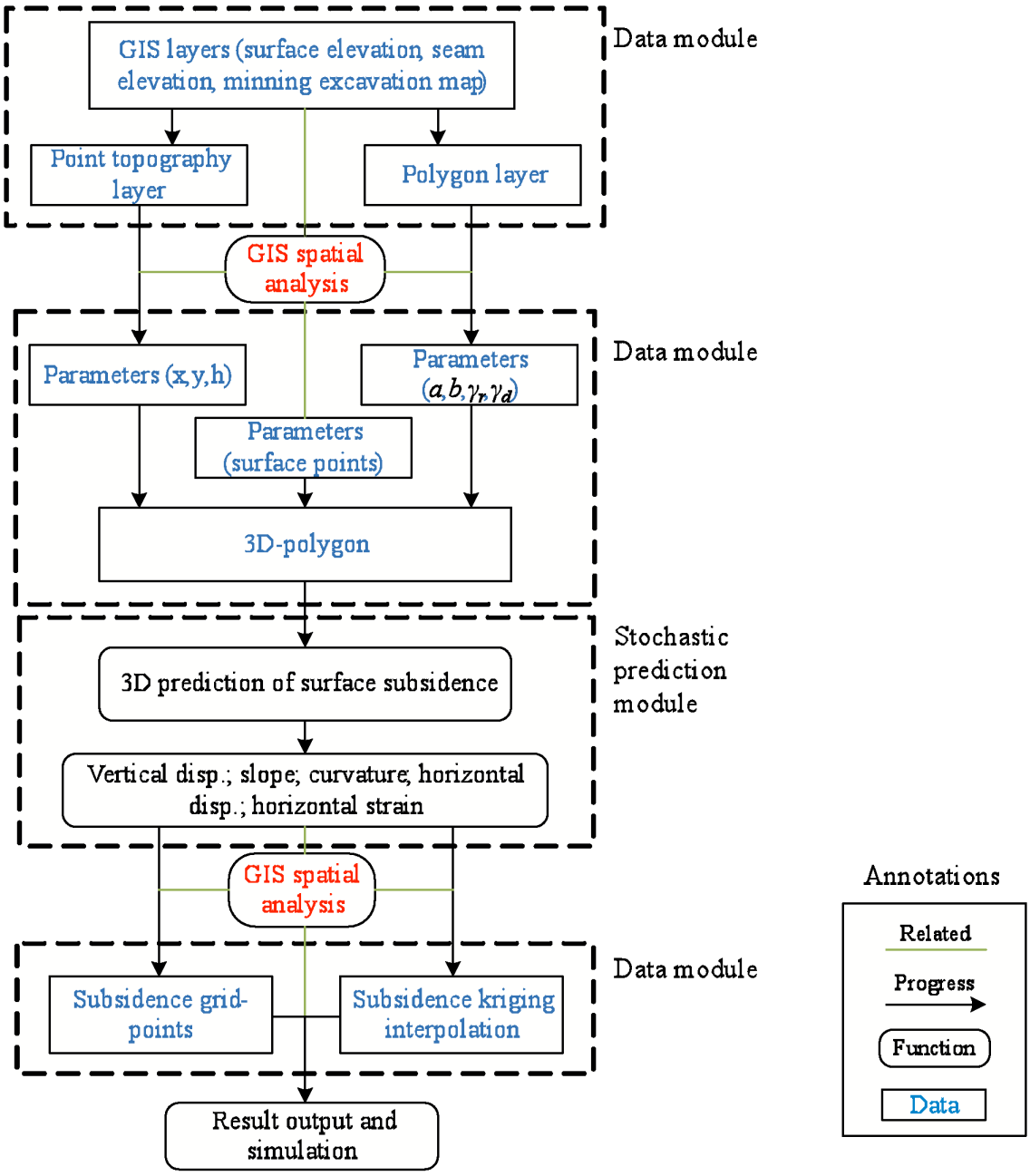

Figure 7: Flow chart of GIS data processing and analyzing for develop 3D extraction model

geometry model of block caving at DOZ and the 3D grid calculation points with interval 20m in x and y direction that have different elevation data is shown in Figure 8 and 9, respectively.

4.2 Parameter estimation using empirical and observed data

Ground movement calculation, simulating the extraction process between 2000 and 2008, were carried out by employing parameters of subsidence factor (a) = 0.1, horizontal movement factor (b) = 0.025, and tangent of draw angle (γ) = 2.14. Those parameters were obtained from the Subsidence Engineering Handbook (SEH 1975) and some measurements by previous study. The effect of the time factor, which expresses time-delayed ground deformation, is not considered in this calculation.

4.3 Prediction of vertical displacement and horizontal strain using GIS

Prediction models calculate the movements of a surface point for an extraction panel in three dimensions. Because an individual point may consists of difference in ground elevation, the use of the 3D prediction model for obtaining the spatial distribution of subsidence is very time-consuming without the GIS as each surface point has to be calculated separately. To overcome the problem of complex geometrical data conversion, the model of subsidence calculation points can be performed within the GIS.

All modules are related to the GIS spatial-analysis function, which is implemented by a GIS component. Figure 9 shows the 3D view of subsidence distribution and horizontal strain distribution resulting from past DOZ mining in stages including from 2000 to 2008. For these spatial simulations, all calculation points were interpolated by using the Kriging interpolation method.

5 Result and discussions

According to the simulation results, the significant influence of horizontal tensile strain at the east side of surface subsidence area grew because of extensive extraction ore was done early in stages including 2001, 2002, and 2003. At the same time, the concentration of tensile strain was identified as the same as the location where huge rock slope failure was occurred at the east side of subsidence area (Figure 9). Moreover, because the distribution of vertical displacement is developed at the terrain slope, the degree of slope becomes steeper than the original slope value in particular at the upper part of slope. Thus, the increasing slope degree may be contributed to the slope instability factor as well. The direct observation for ground elevation change is not yet performed in the site location because of dangerous slope, high elevation (about 4000 m) and hazardous area. Comparing to the result from monitoring topographic change in the vicinity of DOZ using aerial photogrammetry (Setianto *et al.*, 2008), the prediction method using GIS indicates a high value of subsidence. This may be attributed to the fact that, in this model, the effects of mining method, time dependent factor and the condition of caving boundary such as the existence of major faults intercepting the cave surface near the DOZ have not been taken into consideration.

6 Conclusion

Using a GIS prediction model, this paper has calculated ground movement under irregular mining geometry and complex topographic condition. Differential-ground movement characteristics, such as vertical displacement, and horizontal strain, can be computed using GIS effectively. Ground movement in the study area was successfully simulated using empirical and observed data. The calculated result has been used to investigate subsidence-induced rock slope failure resulting from block caving at DOZ.

References

Anon (1975) Subsidence Engineers Handbook, National Coal Board, London.

American Geology Institute (1996) Dictionary of Mining, Mineral, and Related Terms, American Geology Institute in cooperation with the Society for Mining, Metallurgy, and Exploration, 549.

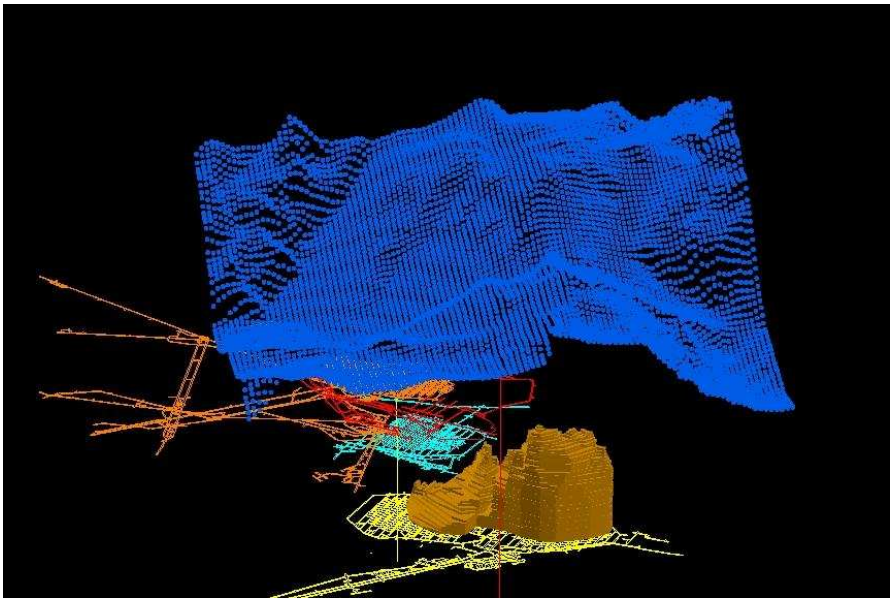

Figure 8: The generated 3D grid points by extracting Digital Elevation Model (DEM) data

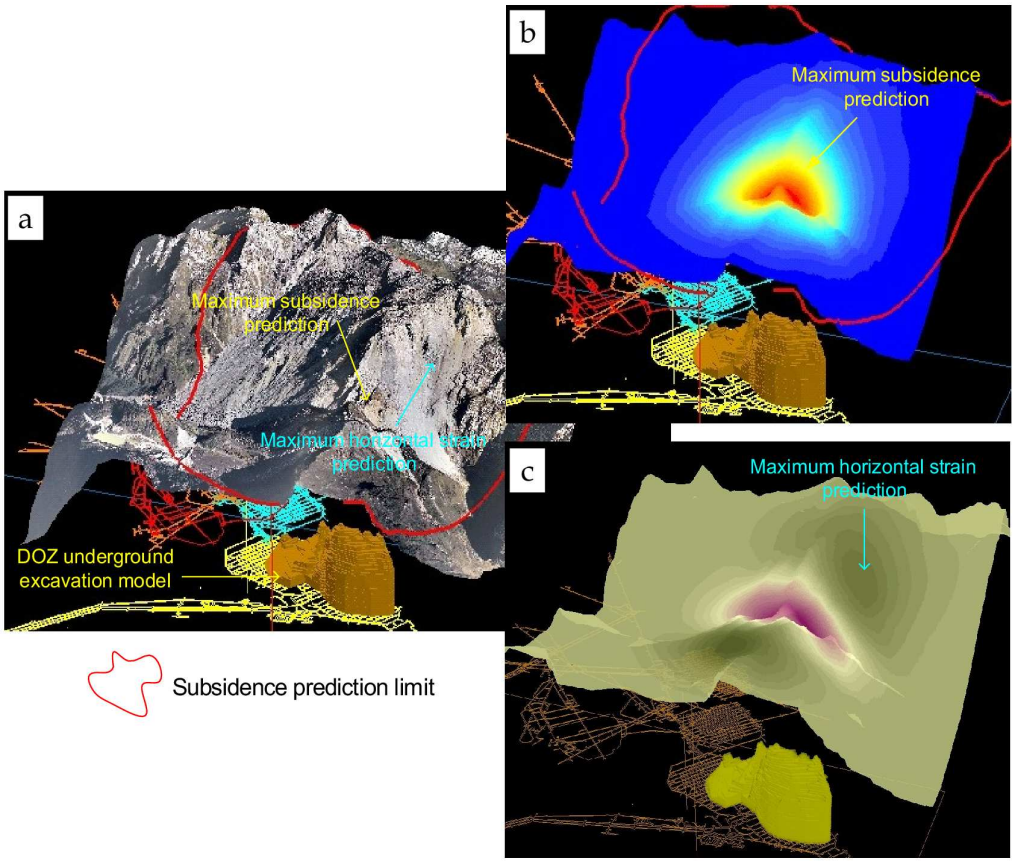

Figure 9: (a) The 3D view of the location of huge rock slope failure of subsidence area which induced by ground movement and the calculated maximum ground movement due DOZ extraction up to 2008 by means of complete extraction: (b) The vertical displacement; (c) The horizontal strain distribution

Berry, D. S. (1964) The ground considered as a transversely isotropic material, Int. J. Rock Mech. Min. Sci. 1, 159-167.

Coutts B.P., Flint D., Belluz N., Susanto H., Edwards A. (1999) Geology of the Deep Ore Zone, Erstberg East Skarn System, Irian Jaya, Proc. PACRIM '99, 539-547.

Flores G., Karzulovic A., Brown E.T. (2004) Current practices and trends in cave mining, MassMin 2004, Santiago, 83-89.

Zhao, D.S., T. Xu, C.A. Tang (2004) Numerical simulation of bed separation of overburden strata induced by mining excavation. Proc. the 3rd ARMS, Kyoto, 475-478.

Esaki, T., I. Djamaluddin, Y. Mitani (2004) Synthesis subsidence prediction method due to underground mining integrated with GIS, Proc. The 3rd ARMS, Kyoto, 147-152.

Whittaker, B.N. and D.J. Reddish (1989) Subsidence occurrence, prediction and control, Elsevier, Amsterdam.

Litwiniszyn, J. (1957) The theories and model research of movements of ground masses, Proc. European Congress on Ground Movement, 202-209.

Setianto A., T. Esaki, Y. Mitani, I. Djamaluddin, H. Ikemi (2008) GIS Analysis of Surface Subsidence Associated with Block Caving Mining at Papua, Indonesia, Proc. Int. Earth Science and Technology, Fukuoka, 275-282.

Szwedzicki T., Widijanto E., Sinaga F. (2004) Propagation of a caving zone, A case study from PT Freeport Indonesia, MassMin 2004, Santiago, 508-512.

